J Mater Sci (2010) 45:1677–1682
DOI 10.1007/s10853-009-4151-y

Study of oxygen reduction on copper applied to the peroxidase-mediated oxidation of methylene blue

**Jaqueline B. de Matos · Marcio José E. M. Cardoso ·
Oswaldo E. Barcia · Guilherme C. G. de Oliveira ·
Eliane D'Elia**

Received: 2 July 2009 / Accepted: 18 December 2009 / Published online: 5 January 2010

Abstract The kinetics of oxygen reduction was studied on copper in tartarate solutions using a rotating disc electrode. The effect of pH on the cathodic reduction was examined. AC impedance and cathodic polarization curves showed that the reaction is partially controlled by mass transport. At high current densities, the limiting current values showed that O_2 is reduced mainly through the four electron pathway. From measurements of density and viscosity and data taken from Levich and Tafel plots, diffusion coefficients for oxygen in tartarate medium were calculated. Peroxidase-mediated oxidation of methylene blue (MB) results using electrogenerated H_2O_2 on copper electrode showed that O_2 reduction reaction occurs in two steps producing the adsorbed intermediate species H_2O_2 by k_2. In the absence of peroxidase, the hydrogen peroxide elimination has to be rapid with $k_3 \gg k_M$. The MB oxidation by lignin peroxidase using electrogenerated H_2O_2 was studied. After 24 h LiP is able to oxide the MB, producing different oxidized forms: azure C and thionine, with yield of 23% and 66%, respectively.

Introduction

The electrochemical reduction of oxygen is an important reaction due to its applications in corrosion studies [1–5], fuel cell technology [6–14] and more recently, the enzymatic mediated oxidation of organic compounds commonly found in industrial waste waters, such as chlorinated phenols and polyaromatic hydrocarbons, using electrogenerated hydrogen peroxide [15–17].

The mechanism of oxygen reduction occurs through two parallel steps, one involving the direct reduction of adsorbed oxygen by k_1 with four electrons and the other involving peroxide intermediate formation by k_3 (Scheme 1). This mechanism was first proposed by Wroblowa et al. using a rotating-ring disc electrode system on gold in alkaline solution [12]. It is important to note that although the involvement of four electrons indicates that direct reduction is occurring, Tarasevich et al. proposed that these conditions would also be found if a rapid elimination of H_2O_2 was present, i.e., $k_3 \gg k_M$ [18].

Oxygen reduction on copper is inhibited by metal oxidation into the $Cu/Cu_2O/CuO$ duplex layer potential region. The Tafel slope is close to -0.3 V/decade, and the reduction proceeds through a CE mechanism [1]. When Cu(I)-complexing electrolytes are employed, the rate constant increases, showing that oxygen reduction can proceed by a CE mechanism and a direct electron transfer mechanism [1]. For copper–nickel alloys in alkaline medium, Ceré et al. [8] found that the oxygen reduction occurs through a sequential mechanism with rapid peroxide consumption.

Peroxidases are oxidative, peroxide-dependent enzymes that catalyze the oxidation of a wide variety of organic and inorganic compounds. The literature shows that the use of hydrogen peroxide in biocatalysis as a co-substrate for peroxidase activity is limited due to its inhibitory effect at high concentrations. One solution for this problem is the use of very low and controlled hydrogen peroxide supplementation, necessary just for the maintenance of an effective peroxidase oxidation level. This can be achieved using H_2O_2 direct pulsated addition or by in situ electrogeneration. The electroenzymatic approach provides a

---

J. B. de Matos · M. J. E. M. Cardoso · O. E. Barcia ·
G. C. G. de Oliveira · E. D'Elia (✉)
Institute of Chemistry, Federal University of Rio de Janeiro, CT,
Cidade Universitária, CEP 21949-900 Rio de Janeiro, Brazil
e-mail: eliane@iq.ufrj.br

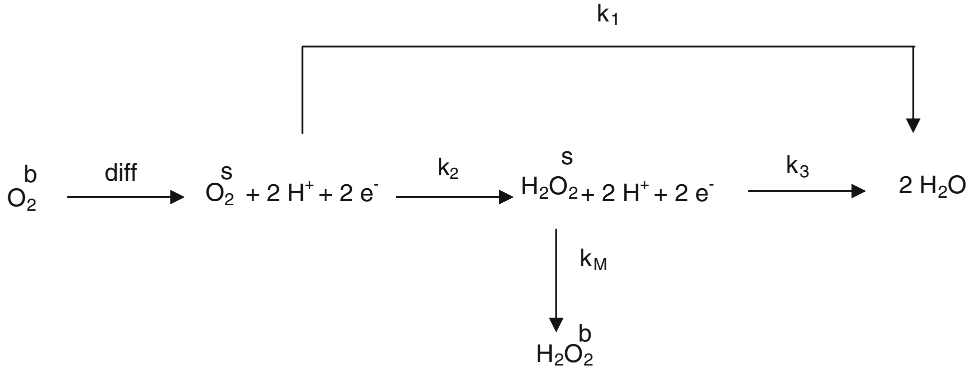

Scheme 1 Model for the electroreduction of O_2 proposed by Wroblowa et al. for gold in alkaline solution [12]; s = adsorbed on the surface; b = in bulk solution

significantly lower and easily controllable hydrogen peroxide formation rate than any other thus far [15–17].

Methylene blue (MB) is a very commonly used dye in the industry. It has many uses in a range of different fields, such as biology and chemistry. In analytical chemistry, it is widely used as a redox indicator. In the industries, colored wastewater is released in textile effluents and poses a potential environmental hazard. Within the ecosystem, this colored wastewater is a dramatic source of pollution, eutrophication, and perturbations in aquatic life. Moreover, a variety of organic chemicals are produced during the dyeing process, and some have been shown to be carcinogenic. With the growing awareness of decreasing available water resources, many methods are being used in wastewater treatment and recycling where MB has been chosen as a model compound [19–22].

To understand the best conditions to produce hydrogen peroxide electrochemically, the objective of this work was to study the mechanism of oxygen reduction on copper in a sodium tartarate aqueous solution in the 2–7 pH range. This pH range was chosen due to the peroxidase stability depending on this parameter. For example, lignin peroxidase (LiP) and horseradish peroxidase (HRP) present maximum activities at 4.0 and 6.0 pH, respectively. The buffer sodium tartarate solution is a convenient medium for studies with Lip as biocatalyser. Moreover, the electrogenerated hydrogen peroxide was applied to the Lip-mediated oxidation of MB in aqueous media.

Experimental

The polarization experiments were carried out in a conventional three-electrode cell. An $Hg/Hg_2SO_4/K_2SO_4$ (sat) electrode was used as the reference electrode (0.641 V versus NHE). All potentials were referenced to this electrode. A long platinum wire was used as the counter electrode. The rotating disc electrode (RDE) was constructed from Cu supplied by Johnson Matthey. The exposed active electrode area was 0.2 cm^2. Prior to the experiments, the electrode was mechanically polished with emery paper to grades 1,000, 1,200, 1,500, and 2,000 and cathodically cleaned at −2.0 V for 3 min.

The current–potential curves were conducted at different rotation rates with a 0.001 V s^{-1} scan rate from the open circuit potential. The AC impedance measurements were carried out at fixed potentials for different rotation rates in the frequency range from 100 kHz to 1.0 MHz with 10 mV of signal amplitude.

All electrochemical measurements were carried out with a Radiometer Analytical—Electrochemistry potentiostat, and the electrode rotation speed was controlled by an analytical rotator (Asservissement Electronique—France).

For values in the pH range 5–7, measurements of density, viscosity, and concentration of dissolved O_2 were performed.

The densities of the solutions were measured with a digital oscillating u-tube density meter (Anton Paar, model DMA 4500) with an uncertainty of 5×10^{-5} g cm^{-3}. For all solutions, the density was measured at least twice. A third measurement was made only if the reproducibility between the two-first previous measurements was greater than 3×10^{-5} g cm^{-3}.

The efflux time of the solutions were measured with Cannon–Fenske viscometer (Schott-Geratle) calibrated and certified by the company that supplies us. For each solution at least 10 repetitions of the efflux time were performed and the results were averaged. The uncertainty in the efflux time was 0.01 s.

The concentration of oxygen was measured using the Winkler method [23, 24].

Studies were conducted at room temperature (23 ± 1 °C). Solutions were prepared from analytical grade reagents and distilled water. The experiments were measured in a naturally oxygen-saturated 0.2 mol L^{-1} tartaric acid ($C_4O_6H_6$) solution containing different concentrations of NaOH, which produced various pH values (2–7).

The MB oxidation was performed in 0.2 mol L^{-1} sodium tartarate solution pH 4.0 containing 33 µmol L^{-1}

MB and 0.55 μmol L^{-1} LiP using galvanostatic polarization ($i = -0.02$ mA) during 24 h at room temperature. The oxidized products analysis was performed by High Performance Liquid Chromatography (HPLC) as described by Ferreira-Leitão et al. [22]. Methylene blue, azure B, azure A, azure C, and thionine, used as standards, were purchased from Sigma. Before the peroxide-mediated oxidation of MB using electrogenerated hydrogen peroxide the buffer solution was purged with pure O2 (5.0 mL $\min^{-1}$) during 30 min.

LiP activity was assayed using veratryl alcohol as substrate [22]. Peroxidase concentration was determined using $\varepsilon 403 = 102$ mM^{-1} cm^{-1}.

Results and discussion

Oxygen reduction mechanism

Figure 1 shows the polarization curves for oxygen reduction on copper in the 2–7 pH range for several rotation frequencies (Ω) of the copper RDE. For all investigated pH values, an increase in rotation frequency caused an increase in the current density. These results are due to the transport of O_2 from solution to the copper surface. However, it was only possible to observe a well-defined diffusion plateau for the 5–7 pH range. The reaction order p was calculated from [13]

$$\log j = \log j_k + p \log(1 - j/j_D) \qquad (1)$$

where j_k is the electrode kinetic current density extrapolated to $\Omega = \infty$, and j and j_D are the measured electrode current density and the diffusion electrode current density, respectively. Figure 2 shows that the slopes of log j versus log $(1 - j/j_D)$ plots are very close to 1.0. The values of p for pH 5, 6, and 7 were 0.98, 1.06, and 1.07, respectively. For pH < 5.0, the current plateau was poorly defined, and relation (1) was not verified. This result is probably due to the proton or water reductions that play a major role in this pH range.

For an electrode reaction under mixed kinetic-diffusion control, the current density is given by [13]

$$j^{-1/p} = j_k^{-1/p} + \frac{0.62 D_{\mathrm{eff}}^{-(2/3)} \upsilon^{1/6}}{nFc_b} j^{(1-1/p)} \Omega^{-1/2}, \qquad (2)$$

where n is the number of electrons, F is the Faraday constant, D is the diffusion coefficient of oxygen, υ is the kinematic viscosity, and c_b is the bulk concentration of oxygen. The concentration of oxygen was measured using the Winkler method. This method consists of determining the concentration level of dissolved gas, using titration after fixing O_2. This value, 1.87×10^{-7} mol cm^{-3}, did not vary with pH. The values of kinematic viscosity (υ) were calculated from the experimentally obtained values of viscosity (η) and density (ρ). These results are shown in Table 1.

Figure 3 shows the $j^{-1/p}$ versus $j^{(1 - 1/p)}\Omega^{-1/2}$ plots. From the average values of the slopes obtained at pH 5.0, using the experimentally determined values from Table 1,

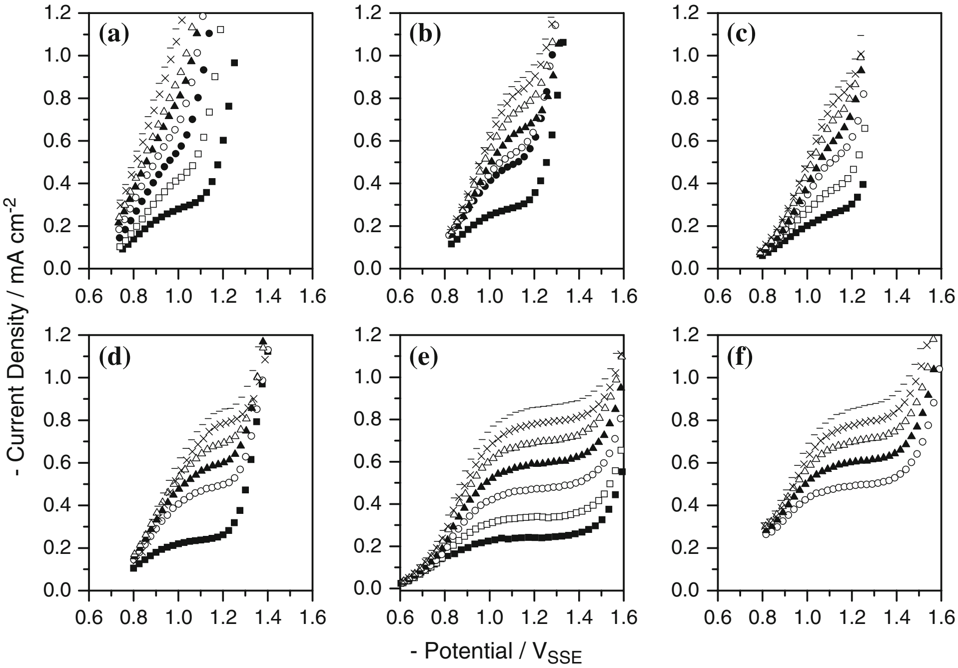

Fig. 1 Polarization curves for O_2 reduction on copper in naturally oxygen-saturated 0.2 mol L^{-1} tartarate medium in the pH range 2–7 at various rotation rates: sweep rate = 1 mV s^{-1}. *Filled square*: 100 rpm; *open square*: 200 rpm; *filled circle*: 300 rpm; *open circle*: 400 rpm; *filled triangle*: 600 rpm; *open triangle*: 800 rpm; *times*: 1000 rpm; *dash*: 1200 rpm. Graphics: **a** pH 2.0; **b** pH 3.0; **c** pH 4.0; **d** pH 5.0; **e** pH 6.0; and **f** pH 7.0

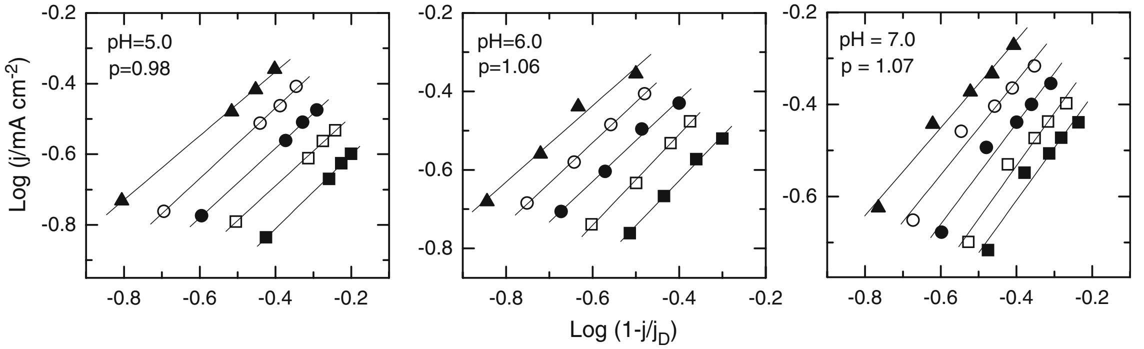

Fig. 2 Reaction order for O_2 reduction on copper in naturally oxygen-saturated 0.2 mol L^{-1} tartarate medium in the pH range 5–7 at potentials of *filled square*: -850 mV_{SSE}; *open square*: -870 mV_{SSE}; *filled circle*: -890 mV_{SSE}; *open circle*: -910 mV_{SSE}; and *filled triangle*: -930 mV_{SSE}

Table 1 Values of kinematic viscosity (υ) calculated from the experimentally obtained values of viscosity (η) and density (ρ)

pH	η (g cm^{-1} s^{-1})	ρ (g cm^{-3})	υ (cm^2 s^{-1})
5.0	9.854×10^{-3}	1.02144	9.647×10^{-3}
6.0	9.845×10^{-3}	1.02176	9.635×10^{-3}
7.0	9.861×10^{-3}	1.02186	9.650×10^{-3}

and assuming $n = 4$, the diffusion coefficient was calculated to be 1.82×10^{-5} cm^2 s^{-1}. This value of D is consistent with the values found in the literature [6] for aqueous media. For pH 6.0 and 7.0, using $D = 1.82 \times 10^{-5}$ cm^2 s^{-1} and the data from Table 1, the values of n were 3.9 and 4.2, respectively. These results confirm the mechanism proposed by Wroblowa et al. for the reduction of O_2 on a surface of gold in alkaline medium. A similar value of n was obtained for oxygen reduction on copper in borax medium [1].

The AC impedance results obtained at different pH, potential, and rotation rate values showed two poorly resolved loops. Figure 4 presents the results for pH 7.0 at -1.2 V. The loop corresponding to the low frequency range is due to mass transport, since its frequency varies

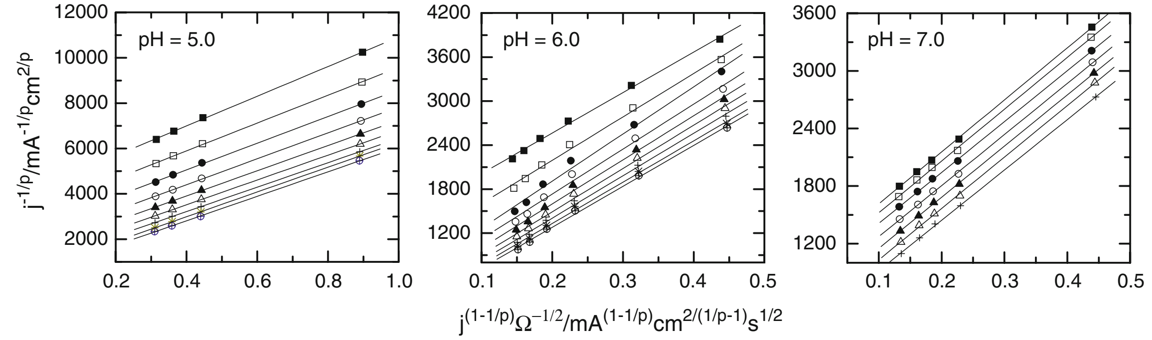

Fig. 3 Koutecky-Levich plots for O_2 reduction on copper in naturally oxygen-saturated 0.2 mol L^{-1} in tartarate medium in the pH range 5–7 at potentials of *filled square*: -810 mV_{SSE}; *open square*: -830 mV_{SSE}; *filled circle*: -850 mV_{SSE}; *open circle*: -870 mV_{SSE}; *filled triangle*: -890 mV_{SSE}; *open triangle*: -910 mV_{SSE}; *cross*: -930 mV_{SSE}; *asterisk*: -950 mV_{SSE}; and *crossed circle*: -970 mV_{SSE}

Fig. 4 AC impedance obtained at -1.2 V for three different rotation rates at pH 7.0

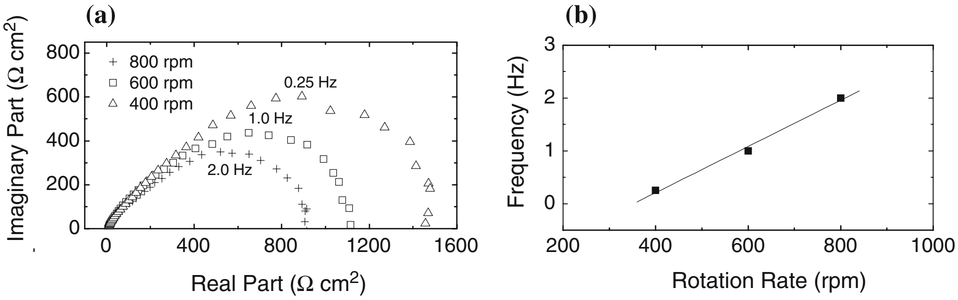

Fig. 5 Chemical structure of methylene blue and *N*-demethylated derivatives

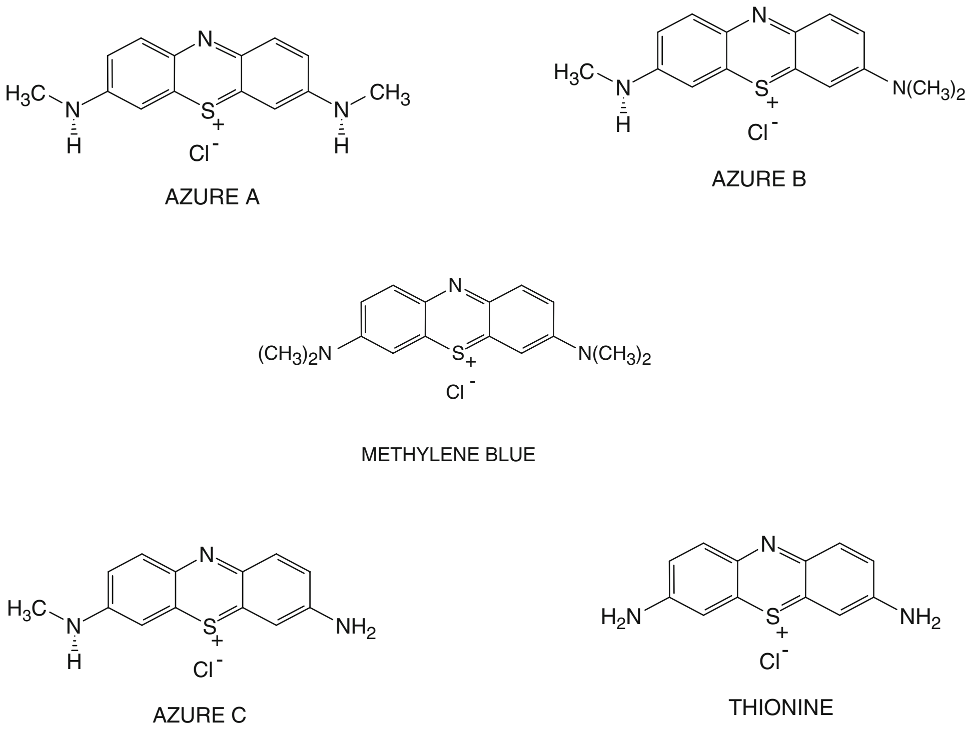

with the rotation rate (Fig. 4a). A linear plot of the characteristic frequency versus rotation rate indicates that the mass transport occurs entirely in the fluid (Fig. 4b). The same results were obtained for pH 5.0 and 6.0. In addition, similar results were obtained by Deslouis et al. for copper in neutral NaCl medium [25]. The loop corresponding to high frequency is due to combination of charge transfer resistance and double layer capacitance.

Electrogeneration of hydrogen peroxide applied to the LiP-mediated oxidation of MB in aqueous media

Figure 5 shows the chemical structures of the MB and their oxidized derivatives. HPLC products analysis from LiP-catalyzed reaction using electrogenerated H_2O_2 by the oxygen reduction on copper electrode for 24 h showed a total conversion of MB in its oxidated products: azure C and thionine. The product percentage contribution was 23% of azure C and 66% of thionine. Although in this study, it was shown that the oxygen reduction mechanism considers four electrons, the LiP-mediated oxidation of MB results showed that O_2 reduction reaction occurs in two steps producing the adsorbed intermediate species H_2O_2 by k_2. In the presence of peroxidase, the enzyme captures the adsorbed hydrogen peroxide on the electrode surface, producing the MB oxidated compounds. In the absence of peroxidase, the hydrogen peroxide elimination has to be very rapid with $k_3 \gg k_M$ as proposed by Tarasevich et al. Under these conditions, $n = 4$ is justified, even using RDE results.

Conclusions

On the basis of the results obtained for the oxygen reduction on copper in tartarate solution, the following points can be concluded:

- in tartarate solution and for a limited pH range (5–7), four electrons are exchanged in the investigated potential range according to the mechanism proposed by Wrolowa et al. [12];
- the order of the investigated reaction is one;
- the mass transport occurs only in the solution and not through an oxide layer;
- for this pH range, the value for the diffusion coefficient obtained by assuming the transference of four electrons was consistent with the values found in the literature;
- the oxygen reduction on copper occurs in two steps producing the adsorbed intermediate species H_2O_2 by k_2 and its elimination has to be very rapid with $k_3 \gg k_M$ in the absence of peroxidase; and
- LiP was able to oxidize the MB in azure C and thionine after 24 h using electrogenerated H_2O_2 on copper electrode, showing a product percentage contribution of 23% and 66%, respectively.

Acknowledgements We are grateful to CAPES/Brazil for the doctoral research grant given to Jaqueline B. de Matos.

References

1. Vazquez MV, Sanchez SR, Calvo EJ, Schiffrin DJ (1994) J Electroanal Chem 374:189
2. Calvo EJ, Schiffrin DJ (1998) J Electroanal Chem 243:171
3. Jin S, Ghali E (1991) J Appl Electrochem 21:247
4. Jin S, Djellab H, Ghali E (1990) Hydrometallurgy 24:53
5. Jin S, Ghali E (1992) Can Met Q 31:259
6. Kinoshita K (1992) Electrochemical oxygen technology. Wiley, New York
7. Brisard G, Bertrand N, Ross PN, Markovic NM (2000) J Electroanal Chem 480:219
8. Ceré S, Vazquez MV, Sanchez SR, Schiffrin DJ (2001) J Electroanal Chem 505:118
9. Markovic NM, Gasteiger HA, Ross PN (1997) J Electrochem Soc 144:1591
10. Markovic NM, Gigur BN, Ross PN (1997) J Phys Chem 101:5405
11. Markovic NM, Adzic RR, Vesovic VB (1984) J Electroanal Chem 165:121
12. Wroblowa HS, Pan YC, Razumney G (1976) J Electroanal Chem 69:195
13. Vesovic V, Annastasijevic N, Adzic RR (1987) J Electroanal Chem 218:53
14. Jiwei L, Jingxia Q, Miao Y, Chen J (2008) J Mater Sci 43:6285. doi:10.1007/s10853-008-2905-6
15. Rotta CEL, Werberich DS, D'Elia E (2008) Electrochem Comm 10:108
16. Rotta CEL, D'Elia E, Bon EPS (2007) Elect J Biotechnol 10:24
17. Rotta CEL, Werberich DS, Contrucci M, D'Elia E (2007) Elect J Biotechnol 10:1
18. Tarasevich MR, Sadkowski A, Yeager E (1983) In: Conway BE, Bockris JOM, Yeager E, Khan SUM, White R (eds) Comprehensive treatise of electrochemistry, vol 7. Plenum Press, New York
19. Yuan R, Guan R, Shen W, Zheng J (2005) J Colloid Interface Sci 282:87–91
20. Yogi C, Kojima K, Takai T, Wada N (2009) J Mater Sci 44:821–827. doi:10.1007/s10853-008-3151-7
21. Ramalho TC, Carvalho HWP, Batista APL, Pérez CA, Gobbi AL (2009) J Mater Sci 44:1029. doi:10.1007/s10853-008-3206-9
22. Ferreira-Leitão VS, Silva JG, Bon EPS (2003) Appl Catal B Environ 42:213
23. Winkler LW (1888) Chem Ber 21:2843
24. Wheatland AB, Smith LJ (1955) J Appl Chem 5:144
25. Delouis C, Tribollet B, Mengoli G, Musiani M (1988) J Appl Electrochem 18:384